SLAYER: Synthetic Lethality Analysis for Enhanced Targeted Therapy Implicates AhR inhibitor as a Target in RB1-Mutant Bladder Tumors

Ziv Cohen[1,2], Ekaterina Petrenko[2], Alma Sophia Barisaac[2], Enas R. Abu-Zhayia[2], Chen Yanovich-Ben-Uriel[2], Nabieh Ayoub[2], and Dvir Aran[1,2,*]

[1]The Taub Faculty of Computer Science, Technion - Israel Institute of Technology, Haifa, Israel
[2]Faculty of Biology, Technion - Israel Institute of Technology, Haifa, Israel
[*]Corresponding author: dviraran@technion.ac.il

Abstract

Synthetic lethality represents a promising therapeutic approach in precision oncology, exploiting genetic vulnerabilities that are exclusive to tumor cells while sparing normal tissues. By targeting non-oncogenic partners of mutated genes that cancers become dependent on, synthetic lethal interactions provide a strategy to selectively kill cancer cells. Here we present SLAYER (Synthetic Lethality AnalYsis for Enhanced taRgeted therapy), a computational pipeline that enables systematic identification and exploration of synthetic lethal interactions (SLIs) by integrating cancer genomic data and genome-wide CRISPR knockout screens. SLAYER associates the DepMap genome-wide CRISPR viability profiles across 808 cancer cell lines with derived gene mutations and mutation-associated pathway enrichment scores to identify potential SLIs. Among the predicted SLIs, inhibition of the aryl hydrocarbon receptor (AhR) was identified as synthetically lethal with RB1 mutations in bladder cancer. We experimentally validated this finding using a commercial AhR inhibitor drug in RB1-proficient and RB1-mutant bladder cancer cell lines. Interestingly, the SLI appears to be indirect, suggesting the RB1 mutational landscape rewires cellular dependencies that confer susceptibility to AhR inhibition during tumor evolution. Our SLAYER framework provides an integrated approach to systematically predict and prioritize synthetic lethal candidates for experimental testing and clinical translation.

Synthetic Lethality, Precision Medicine, CRISPR/Cas9 Screenings

Introduction

Synthetic lethality represents a promising therapeutic strategy in precision oncology by exploiting genetic vulnerabilities exclusive to tumor cells [1]. This approach targets non-oncogenic partners of mutated genes that cancers become dependent on, providing a means to selectively kill cancer cells while sparing normal tissues [2]. Notable examples of clinically relevant synthetic lethal interactions include PARP inhibitors in BRCA-mutated cancers [3] and WEE1 inhibitors in TP53-mutated tumors [4]. By targeting these genetic vulnerabilities, synthetic lethal therapies have shown remarkable success in treating previously intractable cancers.

The Cancer Dependency Map (DepMap, `https://depmap.org/portal/`) is an invaluable resource containing multi-omics data spanning over 1,000 cancer cell lines. This includes genome-wide CRISPR-Cas9 knockout screens that comprehensively probe gene essentiality by measuring cellular viability upon individual gene disruptions. The CRISPR screening data, represented as gene dependency scores, is complemented by genomic profiles such as mutations, copy number variations, and gene expression. A recent study by Chan et al. leveraged this resource to identify WRN as a synthetic lethal target in microsatellite unstable (MSI) versus microsatellite stable (MSS) cancers by comparing cell line subgroups stratified by microsatellite status [5]. Another recent study addressed the need for a systematic method to infer synthetic lethal interactions (SLIs) using DepMap, focusing on identifying potential SLIs in DNA damage response genes [6].

Here, we present a framework called SLAYER (Synthetic Lethality AnalYsis for Enhanced taRgeted therapy) that integrates the multi-dimensional DepMap dataset to systematically identify associations with common cancer mutations and pathway dependencies. By intersecting mutation profiles with CRISPR gene essentiality patterns, our approach pinpoints potential SLIs for experimental validation and therapeutic development. From over 142 predicted SLIs, we experimentally validated AhR inhibition as a therapeutic vulnerability in RB1-mutant bladder cancers, illustrating the ability of our SLAYER pipeline to uncover actionable SLIs with direct clinical relevance.

Results

The SLAYER pipeline is based on integration of multi-dimensional data from the DepMap resource to systematically identify synthetic lethal interactions (SLIs) across cancer types. We analyzed 808 cancer cell lines with complete genomic and transcriptomic profiles alongside CRISPR-Cas9 gene essentiality screens. From the mutational landscapes, we identified 120 commonly mutated genes based on a 5% recurrence threshold across the 808 cell lines spanning 31 cancer types.

Using the DepMap CRISPR-Cas9 knockout viability data, we calculated gene-specific dependency scores and their associations with driver gene mutations to identify potential SLIs through two complementary approaches (Figure 1). This integrated analysis yielded an initial set of 4,332 statistically significant potential SLIs ($p-value < 0.05$) with a delta dependency (DD)-score > 0.2 across both the driver gene-oriented and pathway enrichment-oriented approaches. We then applied stringent filtering criteria to prioritize clinically actionable candidates. First, we filtered for partner genes amenable to therapeutic targeting by cross-referencing against the DepMap PRISM repurposing data, retaining only SLIs where the partner gene is inhibitable by an existing drug or compound. Next, we filtered for SLIs involving driver gene mutations with a population frequency greater than 15% based on TCGA data in cBioPortal. This ensures the SLIs are applicable to a sufficiently broad patient population. After this multi-step filtering process focused on statistical significance, effect size, druggability, and clinical relevance, we identified a refined set of 142 high-confidence, actionable potential SLIs for further prioritization and experimental validation (Figure 2 and Supplementary Table 1).

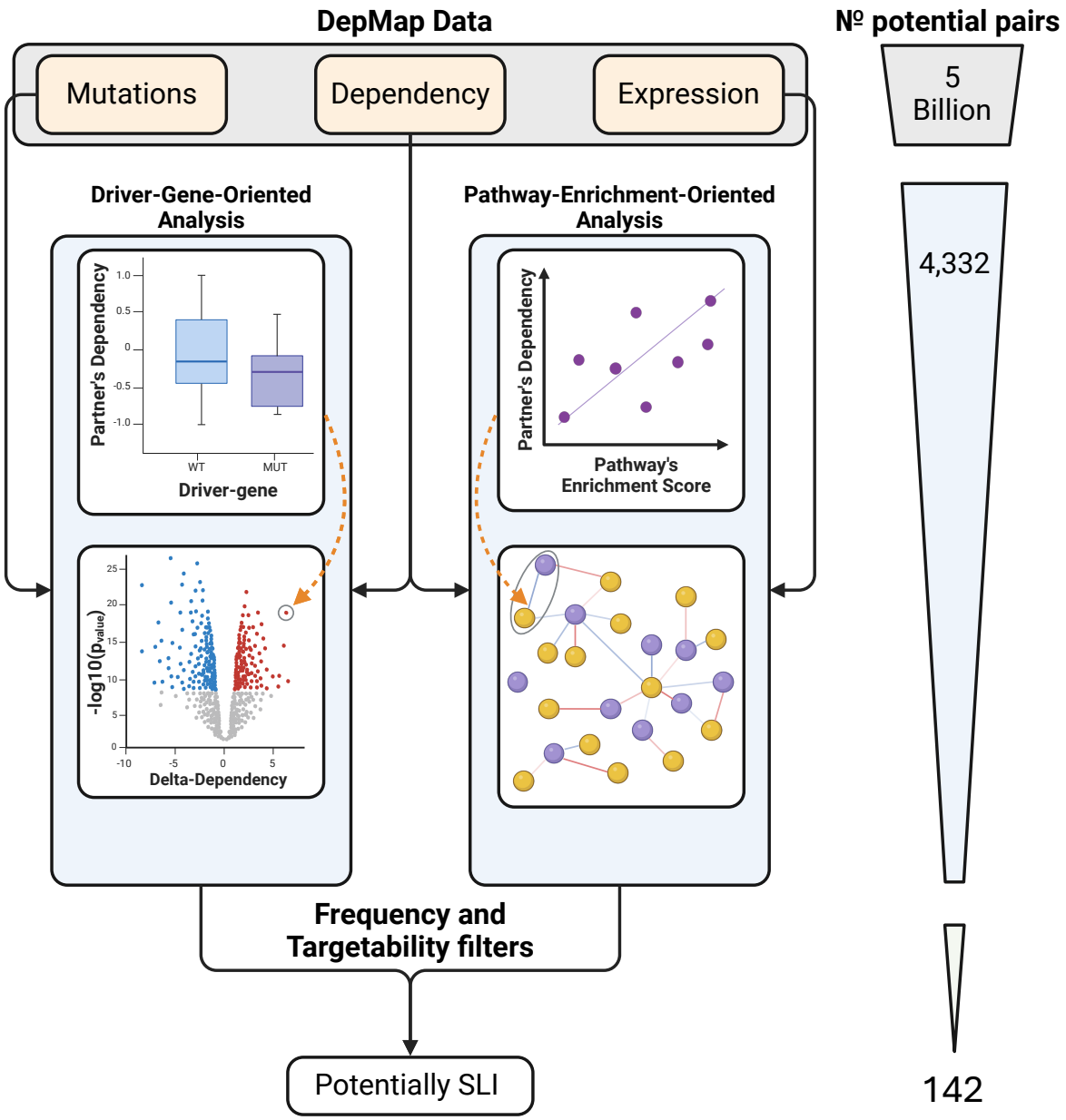

Figure 1: **Schematic overview of the SLAYER methodology.** Data from the DepMap portal, including mutations, gene dependencies, and expression profiles across 808 cancer cell lines, were integrated using two complementary approaches: (i) a driver gene-oriented analysis associating gene dependencies with driver mutations, and (ii) a pathway enrichment-oriented analysis connecting gene dependencies with mutation-associated pathway activities. Putative SLIs were identified from each approach and further filtered based on the driver gene mutation frequency in the patient population and druggability of the partner gene. From an initial 5 billion possible gene pairs, 4,332 statistically significant SLI candidates were identified, which were then refined to a set of 142 high-confidence, actionable SLIs based on effect size, targetability, and clinical relevance filters.

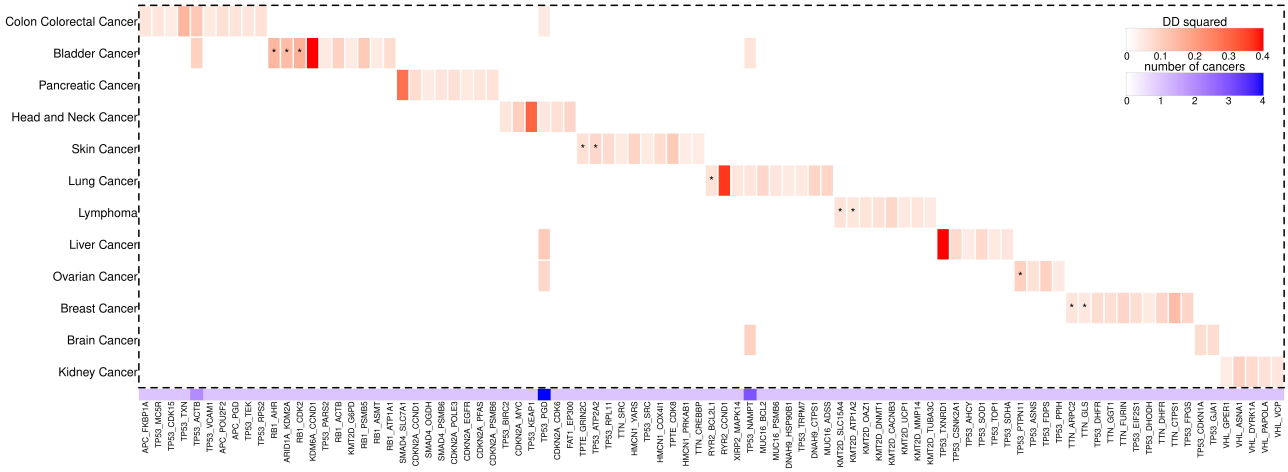

Figure 2: **Potential synthetic lethal interactions across cancer types.** The heatmap displays the top 10 most significant SLIs identified for each cancer type in the analysis. The red color scale corresponds to the delta dependency (DD) score, representing the difference in gene essentiality between the mutant and wildtype groups. The blue bar at the bottom indicates the number of cancer types where the SLI was determined as statistically significant. SLIs with a $p - value < 0.001$, are marked with an asterisk.

Examining the top significant SLIs, we noticed that many of them have been previously implicated or identified in STRING-db (Table 1), a database that integrates known and predicted protein-protein interactions from numerous sources including experimental data, computational predictions, and public literature mining. Notably, one of the top SLIs (STK11-ATP1A1) has been experimentally validated as a synthetic lethal interaction in vivo, while another (RYR2-BCL2L1) was previously implicated as a potential SLI. Furthermore, 8 out of the top 14 most significant SLIs exhibited evidence of the gene pairs co-occurring or interacting based on STRING-db annotations.

Pair	Cancer Type	Driver's Frequency	P-value	DD	External Validation
TPTE-GRIN2C	Skin	22.1%	1.4e-09	0.25	None
STK11-ATP1A1	Lung	28.0%	7.9e-07	0.36	Validated SLI *in-vivo*[7]
TTN-ARPC2	Breast	16.6%	1.1e-04	0.23	IDC
RB1-AHR	Bladder	16.8%	2.2e-04	0.39	ED
ARID1A-KDM2A	Bladder	25.7%	3.0e-04	0.37	CE
KEAP1-ATP1A1	Lung	44.4%	3.1e-04	0.41	None
TTN-GLS	Breast	16.6%	4.1e-04	0.22	None
KMT2D-SLC15A4	Lymphoma	30.8%	4.4e-04	0.24	None
SMARCA4-EP300	Lung	15.7%	4.5e-04	0.24	ED*
RB1-CDK2	Bladder	16.8%	4.6e-04	0.40	ED
TP53-PTPN11	Ovarian	91.6%	4.6e-04	0.31	CE
RYR2-BCL2L1	Lung	39.6%	4.7e-04	0.24	Potential SLI[8]
KMT2D-ATP1A2	Lymphoma	30.8%	6.7e-04	0.23	IDC
TP53-ATP2A2	Skin	15.9%	7.6e-04	0.29	IDC

Table 1: **Top potential synthetic lethal interactions.** ED - Experimentally Determined, CE - co-expression, IDC - Indirect connection. * Co-mentioned in the context of SLIs [9, 10].

To systematically evaluate the biological relevance of our predicted SLIs, we cross-validated the entire set of 142 SLIs against STRING-db interactions across all cancer types (Figure 3). Remarkably, this analysis revealed a 14.5% validation rate for the SLIs compared to only 0.25-0.55% for random pairs of driver genes and partner genes. This striking 30 to 60-fold enrichment underscores the ability of our multi-dimensional approach to pinpoint biologically meaningful SLIs with strong literature support and highlights the putative

clinical significance of the top candidates.

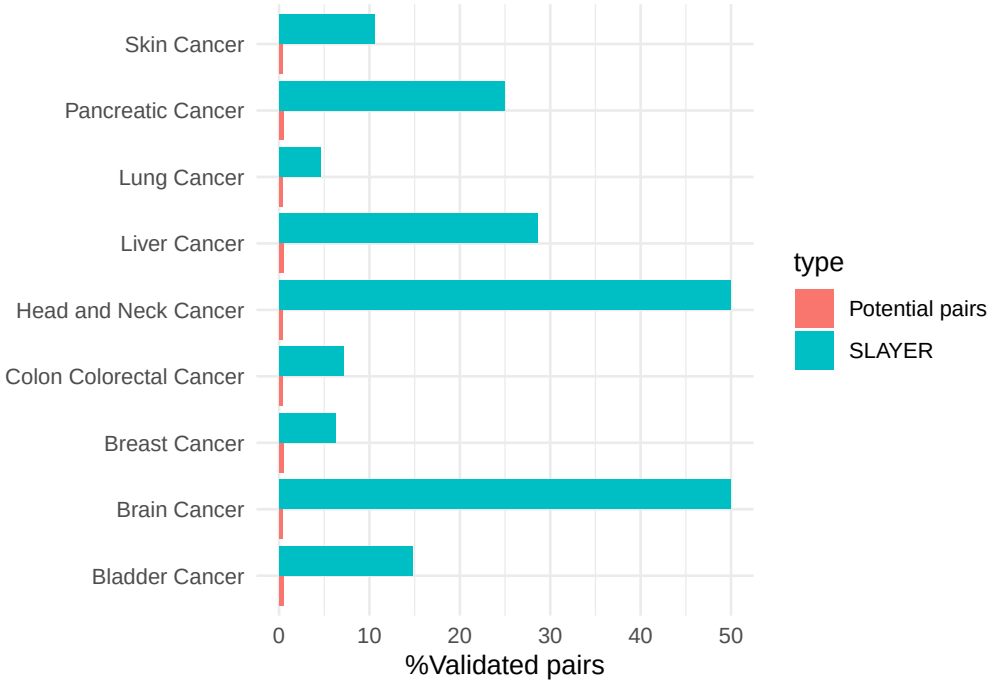

Figure 3: **Validation of predicted synthetic lethal interactions against STRING-db database**. Bar plots show the percentage of gene pairs from the SLAYER analysis that exhibited evidence of interaction or co-occurrence in the STRING-db database, which integrates known and predicted protein associations from multiple sources. The blue bars represent the percentages for the 142 high-confidence SLIs identified by SLAYER, while the red bars indicate the background percentages when analyzing all possible pairwise combinations of driver genes and genes across the different cancer types.

In bladder cancer, our analysis focused on 46 cell lines harboring 7 recurrent driver mutations (Figure 4A; Similar analyses for another cancer types are available in Supplementary Figures 1-2). The top SLIs implicated ARID1A mutant sensitivity to KDM2A knockout and two potential vulnerabilities in RB1 mutant tumors through synthetic lethality with AhR and CDK2 inhibition (Figure 4B-C). RB1 mutations were observed in 18.9% of the bladder cancer cohort, consistent with 16.8% prevalence in TCGA patient samples. Pathway enrichment analysis confirmed associations between AHR knockout dependency and RB1-related signatures, prompting experimental validation of this SLI (Figure 4D-E).

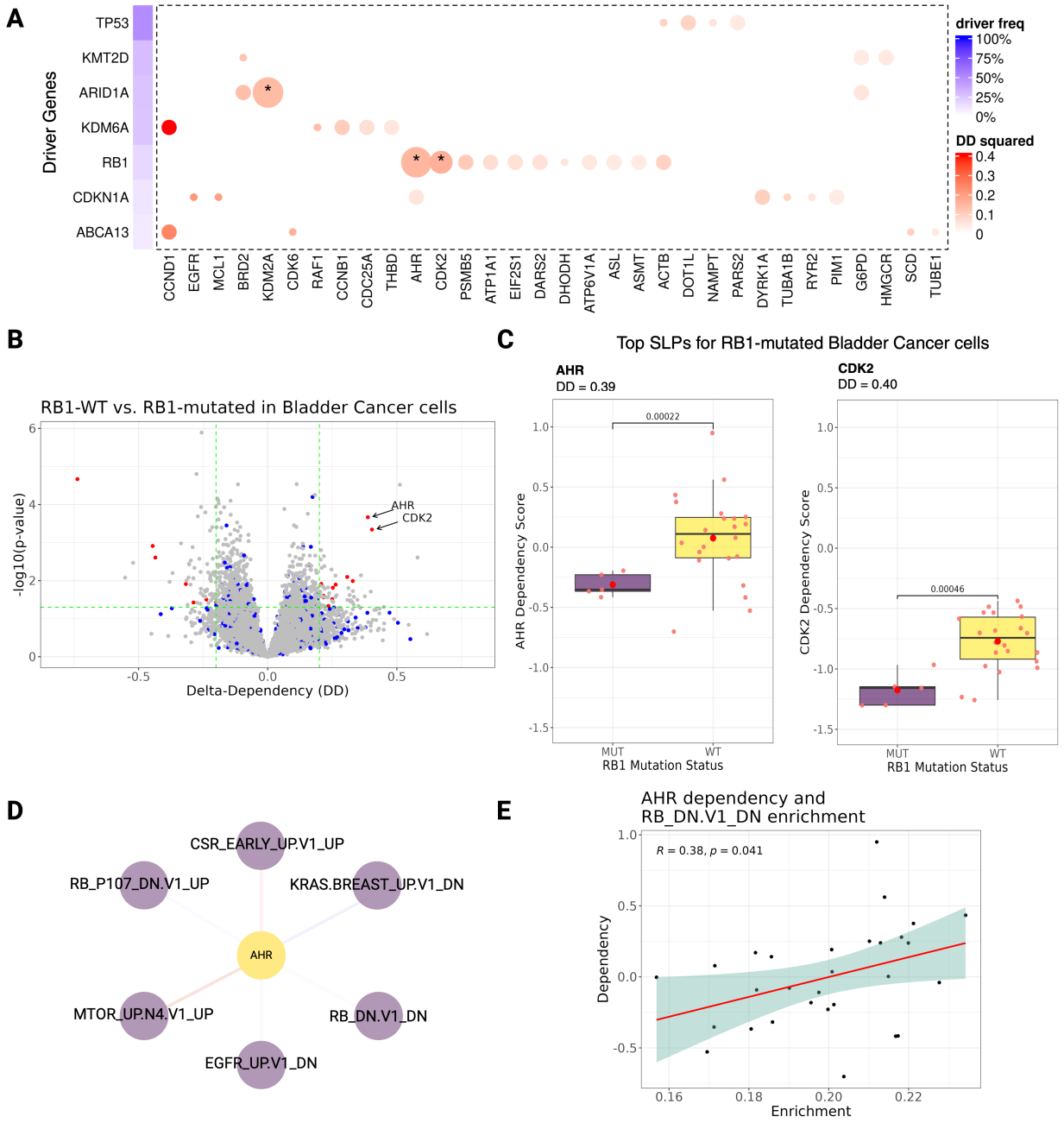

Figure 4: **Potential synthetic lethal interactions in bladder cancer. A.** Heatmap depicting the top synthetic lethal interaction (SLI) pairs in bladder cancer, with redder colors indicating higher delta dependency scores. Similar heatmaps for each of the cancer types are available in Supplementary Figure 1. **B.** Volcano plot showing all potential synthetic lethal interactions for the RB1 mutation, with AHR and CDK2 identified as the top-ranking candidates based on delta dependency (x-axis) and statistical significance (-log10 p-value on y-axis). More examples in Supplementary Figure 2. **C.** Boxplots illustrating the separation in gene dependency scores between RB1 wild-type and RB1 mutant bladder cancer cell lines for the AHR and CDK2. **D.** Dependency network for AHR in bladder cancer, highlighting edges that connect these genes to RB1-associated pathways. **E.** Correlation plot between the dependency scores of AHR and the enrichment of RB1-related pathway across the cell lines.

For experimental testing, we treated the RB1 wild-type bladder cancer cell line T24 and RB1 mutant line 5637 with the AhR inhibitor drug BAY-2416964. Strikingly, the RB1 mutant 5637 cells exhibited significantly increased susceptibility to AhR inhibition compared to the RB1 wild-type T24 cells that remained viable (Figure

5A). Further, BAY-2416964 treatment did not impact the viability of non-cancerous RPE primary cells (Figure 5B), confirming the synthetic lethality between AhR inhibition and RB1 mutation is specific to cancer contexts. Interestingly, depletion of Rb1 in T24 cells did not affect cellular viability following BAY-2416964 treatment (Figure 5C).

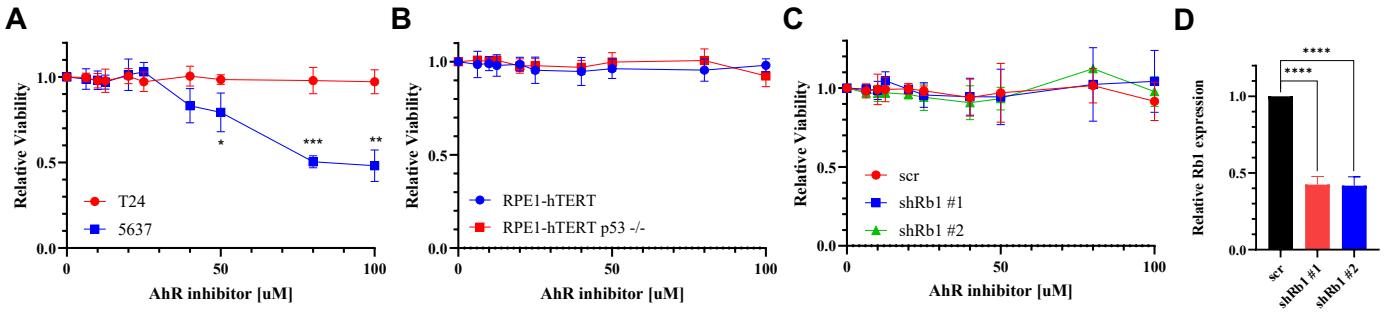

Figure 5: **Synthetic lethality between RB1 and AhR in bladder cancer. A.** Short-term cell viability assay in T24 and 5637 cells treated with increasing concentrations of BAY-2416964. Cell viability was measured 24 hr after drug treatment. Data are presented as mean ± s.d. (n=3). *P < 0.05;**P < 0.01;***P < 0.001 . **B.** Short-term cell viability assay in p53 WT and p53 null RPE1-hTERT cells treated with increasing concentrations of BAY-2416964. Cell viability was measured 24 hr after drug treatment. Data are presented as mean ± s.d. (n=3). **C.** Short-term cell viability assay in T24 cells expressing either scramble shRNA or shRNA targeting Rb1 and treated with increasing concentrations of BAY-2416964. Cell viability was measured 72 hr after drug treatment. Data are presented as mean ± s.d. (n=3). **D.** Quantitative RT-qPCR analysis of Rb1 knockdown in indicated T24 cell lines. ****P < 0.0001.

Discussion

In this study, we developed SLAYER, an integrated computational framework that systematically mines multi-omics data from the DepMap cancer cell line resource to nominate and prioritize potential synthetic lethal interactions (SLIs) associated with recurrent driver mutations across multiple cancer types. Our approach combines complementary techniques analyzing mutational patterns alongside CRISPR gene essentiality profiles as well as pathway enrichment signatures linked to differential gene dependencies. After stringent filtering based on statistical significance, effect size, druggability, and clinical relevance of mutations, we identified a prioritized set of 142 high-confidence SLI predictions.

A top-predicted SLI involved inhibition of the aryl hydrocarbon receptor (AhR) as a therapeutic vulnerability in RB1-mutant bladder cancers. Through experimental validation in isogenic bladder cancer cell line models, we confirmed that RB1 mutant cells exhibited significantly increased susceptibility to an AhR inhibitor drug compared to RB1 wild-type counterparts. This finding holds promise for repurposing AhR inhibitors currently under clinical investigation as a potential therapy for the subset of bladder cancer patients harboring RB1 mutations. Interestingly, further experiments with RB1 knockdown cell lines suggest the synthetic lethality between AhR and RB1 is likely an indirect relationship, potentially driven by the downstream transcriptional consequences and pathway rewiring resulting from RB1 loss-of-function during tumor evolution.

While the current study provides compelling evidence for several high-priority SLI associations such as RB1-AhR in bladder cancer, additional experimental validation and mechanistic investigations are warranted given the inherent limitations of computational predictions from cancer cell line data. Differences in genetic backgrounds, ex vivo culture conditions, and interactions within the tumor microenvironment may influence the manifestation of SLIs in vivo. Nonetheless, our multi-layered SLAYER approach offers a powerful framework to systematically explore the vast mutational landscape across cancers and nominate putative SLIs for therapeutic research and drug repurposing opportunities.

In summary, SLAYER represents a comprehensive methodology integrating complementary perspectives on cancer dependencies to uncover potential SLIs with a strong biological foundation. The clinical translation of

these predictions, as demonstrated by the validation of RB1-AhR synthetic lethality, highlights the capacity of SLAYER to facilitate the discovery of tailored therapeutic strategies that leverage tumor-specific genetic vulnerabilities. With numerous additional high-scoring SLI candidates spanning multiple cancer types, SLAYER offers an expansive resource for future validation studies aimed at delivering on the promise of precision oncology.

Methods

Data availability

This study utilized multi-omics data from the Cancer Dependency Map (DepMap, `https://depmap.org/portal/`) portal, comprising 808 cancer cell lines spanning 31 tissue types (as of DepMap 21Q1 release). We obtained gene expression profiles (RNA-seq data), mutation annotations (from DNA-seq), copy number alterations, and gene dependency scores from genome-scale CRISPR-Cas9 essentiality screens conducted in these cell lines.

Driver Gene-Oriented Analysis

We began by removing hyper-mutated cell lines harboring over 100 putative damaging mutations based on mutation annotation files. Altogether, we excluded 234 cell lines. To define driver genes, we identified genes with non-silent mutations (missense, nonsense, frameshift, or splice site) at $\geq 5\%$ recurrence across all cell lines or across all cell lines of a specific cancer type. For each driver gene, cell lines were stratified into mutant and wild-type groups based on the driver mutation status. Then, for each gene, we calculated the difference in mean gene dependency between the two groups, defined as the delta dependency (DD) score:

$$DD_{g,dg} = \overline{dependency_g \text{ in } WT_{dg}} - \overline{dependency_g \text{ in } MUT_{dg}}$$

A two-sample t-test was applied to assess the significance of dependency differences. Candidate synthetic lethal interactions (SLIs) were identified for driver-gene partners with DD > 0.2 and p-value < 0.05 after Benjamini-Hochberg correction.

Pathway Enrichment-Oriented Analysis

We compiled 189 canonical oncogenic pathway gene signatures from the Molecular Signatures Database (MSigDB, C6 collection) [11, 12]. For each cell line, these pathway genesets were scored using single-sample gene set enrichment analysis (ssGSEA) based on the gene expression data [13]. We then calculated the Pearson correlation between each gene's dependency score and the pathway enrichment scores across all cell lines. A weighted bipartite graph was constructed linking genes to pathways, with edge weights corresponding to the correlation magnitude. Edges were filtered using a threshold of $|r| > 0.5$ and colored based on correlation sign (red=positive, blue=negative), with transparency scaled by:

$$\sigma(w) = 1 - \frac{1}{1+e^{20(|w|-0.6)}}$$

The breadth-first search (BFS) algorithm identified potential mediated relationships connecting driver gene mutations to partner gene dependencies through intermediate pathway nodes.

SLI filtering

The predicted SLIs were filtered to retain those most relevant for clinical translation. SLIs involving driver genes with a mutation frequency = 15% across TCGA patient samples (tested using cBioPortal) were excluded to focus on recurrent events. Additionally, we filtered for druggability by retaining only SLIs where the partner gene is amenable to therapeutic targeting based on the DepMap PRISM repurposing data (https://depmap.org/repurposing/).

Driver-genes' frequency filteration

To filter our SLIs collection, we omitted pairs in which the driver-gene was mutated in less than 15% of the patient population. To achieve this, we used the data generated by the TCGA network (https://www.cancer.gov/tcga), available on cBioPortal (https://www.cbioportal.org).

STRINGdb validation

To evaluate literature support, we queried STRINGdb (version 11.5) [14] to assess what fraction of the predicted SLIs exhibit known or predicted protein-protein associations, co-mentions in publications, or any evidence of functional interactions cataloged in this database.

Experimental validation of the SLI between RB1 and AhR in bladder cancer

Cell lines and cell culture

T24 and 5637 cell lines were grown in RPMI-1640 medium (Gibco) supplemented with 10% heat-inactivated FBS, 2 mM L-glutamine and 100 mg/ml penicillin/streptomycin. RPE1-hTERT wild-type and p53 -/- cell lines were grown in Dulbecco's modified Eagle's medium (Gibco) supplemented with 10% heat-inactivated FBS, 2 mM L-glutamine and 100 mg/ml penicillin/streptomycin.

Lentiviral transduction

Lentiviral particles were generated by co-transfecting HEK293T cells plated in 10cm plates with 1.64pmol target vector, together with 1.3pmol psPAX2 (Addgene #12260) and 0.72pmol pMD2.G (Addgene #12259) using 3:1 μg PEI to μg DNA ratio. Media containing the viral particles were collected 48 hr post-transfection and filtered with 0.45 μm filters. The indicated cell lines were transduced with the lentiviral particles in the presence of 10μg/ml polybrene (Sigma-Aldrich H9268). At 48 hr post-infection, transduced cells were selected using the appropriate antibiotics.

Short hairpin RNA (shRNA) knockdown

shRNA oligonucleotides directed against RB1 were annealed and cloned into pLKO-puro lentiviral vector (Addgene #10878) digested with EcoRI and AgeI. Lentiviral particles were generated as described above and used to transduce T24 cells, followed by selection with 1μg/ml puromycin (Invivogen #ant-pr) for 3 days. Cells were maintained in complete medium in the presence of 0.6μg/ml puromycin. Gene expression knockdown was validated by RT-qPCR. The shRNA and qPCR primer sequences used in this study are included in Supplementary Table 2.

RNA isolation and qPCR

Total RNA was isolated from cells using the TRIzol reagent according to the manufacturer's instructions (Sigma). 1μg RNA was used for cDNA synthesis using the qScript cDNA Synthesis Kit (Quanta) with random primers. Real-time qPCR for measuring mRNA levels was performed using Step-One-Plus real-time PCR System (Applied Biosystems) and the Fast SYBR Green Master mix (Applied Biosystems) with three technical repeats for each PCR. Data analysis and quantification were performed using StepOne software V2.2 supplied by Applied Biosystems. Primer sequences used for qPCR are included in Supplementary Table 2.

AhR inhibitor

BAY-2416964 was purchased from Selleckchem.

Short-term growth delay assay

For determining drug sensitivity, cells were seeded in 96-well plates in duplicates at a density of 3,000-7,500 cells per well. 24 hr post-seeding, BAY-2416964 was added at the indicated concentrations. Cell viability was measured at the indicated timepoints using the CellTiter 96® AQueous One Solution Cell Proliferation Assay (Promega) following the manufacturer's protocol, and absorbance was measured using Epoch Microplate Spectrophotometer (BioTek). Cell viability was normalized to the viability of untreated cells.

Declarations

Data and code availability

All data used in this study is publicly available at the DepMap portal. The code developed in this study is available at `https://github.com/zivc888/SLICE`.

Authors Contribution

The authors confirm their contribution to the paper as follows: study conception and design: DA; algorithm development: ZC; analysis and interpretation of results: ZC & DA; experimental validation: CYBU, ASB, EAZ & NA; draft manuscript preparation: ZC, EP & DA. All authors reviewed the results and approved the final version of the manuscript.

Acknowledgments

We thank Hinanit Kolati for generously sharing cell lines. DA is supported by the Azrieli Faculty Fellowship. ASB is supported by Joan and Irwin Jacobs fellowship. NA is supported by the Neubauer Family foundation. We thank the Aran Lab members for helpful comments.

Funding Statement

Research in the Aran lab is supported by grant from the Israel Science Foundation (1543/21). Research in the Ayoub lab is supported by grants from the Israel Science Foundation (2511/19) and Israel Cancer Research Fund (22-110-PG).

Competing Interests Statement

DA reports consulting fees from Carelon Digital Platforms.

References

[1] Joo Sang Lee, Avinash Das, Livnat Jerby-Arnon, Rand Arafeh, Noam Auslander, Matthew Davidson, Lynn McGarry, Daniel James, Arnaud Amzallag, Seung Gu Park, Kuoyuan Cheng, Welles Robinson, Dikla Atias, Chani Stossel, Ella Buzhor, Gidi Stein, Joshua J. Waterfall, Paul S. Meltzer, Talia Golan, Sridhar Hannenhalli, Eyal Gottlieb, Cyril H. Benes, Yardena Samuels, Emma Shanks, and Eytan Ruppin. Harnessing synthetic lethality to predict the response to cancer treatment. *Nature Communications*, 9(1), 12 2018.

[2] John L Hartman, Barbara Garvik, and Lee Hartwell. Principles for the Buffering of Genetic Variation. *Science*, 291(5506):1001–1004, 2 2001.

[3] Christopher J. Lord and Alan Ashworth. PARP inhibitors: Synthetic lethality in the clinic, 3 2017.

[4] Jiahao Hu, Jiasheng Cao, Win Topatana, Sarun Juengpanich, Shijie Li, Bin Zhang, Jiliang Shen, Liuxin Cai, Xiujun Cai, and Mingyu Chen. Targeting mutant p53 for cancer therapy: direct and indirect strategies, 12 2021.

[5] Edmond M. Chan, Tsukasa Shibue, James M. McFarland, Benjamin Gaeta, Mahmoud Ghandi, Nancy Dumont, Alfredo Gonzalez, Justine S. McPartlan, Tianxia Li, Yanxi Zhang, Jie Bin Liu, Jean Bernard Lazaro, Peili Gu, Cortt G. Piett, Annie Apffel, Syed O. Ali, Rebecca Deasy, Paula Keskula, Raymond W.S. Ng, Emma A. Roberts, Elizaveta Reznichenko, Lisa Leung, Maria Alimova, Monica Schenone, Mirazul Islam, Yosef E. Maruvka, Yang Liu, Jatin Roper, Srivatsan Raghavan, Marios Giannakis, Yuen Yi Tseng, Zachary D. Nagel, Alan D'Andrea, David E. Root, Jesse S. Boehm, Gad Getz, Sandy Chang, Todd R. Golub, Aviad Tsherniak, Francisca Vazquez, and Adam J. Bass. WRN helicase is a synthetic lethal target in microsatellite unstable cancers. *Nature*, 568(7753):551–556, 4 2019.

[6] Salvatore Benfatto, Özdemirhan Serçin, Francesca R. Dejure, Amir Abdollahi, Frank T. Zenke, and Balca R. Mardin. Uncovering cancer vulnerabilities by machine learning prediction of synthetic lethality. *Molecular Cancer*, 20(1), 12 2021.

[7] Nayoung Kim, Hwa Young Yim, Ningning He, Cheol Jung Lee, Ju Hyun Kim, Jin Sung Choi, Hye Suk Lee, Somin Kim, Euna Jeong, Mee Song, Sang Min Jeon, Woo Young Kim, Gordon B. Mills, Yong Yeon Cho, and Sukjoon Yoon. Cardiac glycosides display selective efficacy for STK11 mutant lung cancer. *Scientific Reports*, 6, 7 2016.

[8] Tim Vervliet, Irma Lemmens, Elien Vandermarliere, Elke Decrock, Hristina Ivanova, Giovanni Monaco, Vincenzo Sorrentino, Nael Nadif Kasri, Ludwig Missiaen, Lennart Martens, Humbert De Smedt, Luc Leybaert, Jan B. Parys, Jan Tavernier, and Geert Bultynck. Ryanodine receptors are targeted by anti-apoptotic Bcl-XL involving its BH4 domain and Lys87 from its BH3 domain. *Scientific Reports*, 5, 4 2015.

[9] D. Morel, G. Almouzni, J. C. Soria, and Sophie Postel-Vinay. Targeting chromatin defects in selected solid tumors based on oncogene addiction, synthetic lethality and epigenetic antagonism, 2 2017.

[10] Hideaki Ogiwara, Mariko Sasaki, Takafumi Mitachi, Takahiro Oike, Saito Higuchi, Yuichi Tominaga, and Takashi Kohno. Targeting p300 addiction in CBP-deficient cancers causes synthetic lethality by apoptotic cell death due to abrogation of MYC expression. *Cancer Discovery*, 6(4):430–445, 4 2016.

[11] Aravind Subramanian, Pablo Tamayo, Vamsi K Mootha, Sayan Mukherjee, Benjamin L Ebert, Michael A Gillette, Amanda Paulovich, Scott L Pomeroy, Todd R Golub, Eric S Lander, and Jill P Mesirov. Gene set enrichment analysis: A knowledge-based approach for interpreting genome-wide expression profiles. *PNAS*, 2005.

[12] Arthur Liberzon, Chet Birger, Helga Thorvaldsdóttir, Mahmoud Ghandi, Jill P. Mesirov, and Pablo Tamayo. The Molecular Signatures Database Hallmark Gene Set Collection. *Cell Systems*, 1(6):417–425, 12 2015.

[13] Ming Yi, Dwight V. Nissley, Frank McCormick, and Robert M. Stephens. ssGSEA score-based Ras dependency indexes derived from gene expression data reveal potential Ras addiction mechanisms with possible clinical implications. *Scientific Reports*, 10(1), 12 2020.

[14] Damian Szklarczyk, Andrea Franceschini, Stefan Wyder, Kristoffer Forslund, Davide Heller, Jaime Huerta-Cepas, Milan Simonovic, Alexander Roth, Alberto Santos, Kalliopi P. Tsafou, Michael Kuhn, Peer Bork, Lars J. Jensen, and Christian Von Mering. STRING v10: Protein-protein interaction networks, integrated over the tree of life. *Nucleic Acids Research*, 43(D1):D447–D452, 1 2015.

Figure Legends

Figure 1. Schematic overview of the SLAYER methodology.

Data from the DepMap portal, including mutations, gene dependencies, and expression profiles across 808 cancer cell lines, were integrated using two complementary approaches: (i) a driver gene-oriented analysis associating

gene dependencies with driver mutations, and (ii) a pathway enrichment-oriented analysis connecting gene dependencies with mutation-associated pathway activities. Putative SLIs were identified from each approach and further filtered based on the driver gene mutation frequency in the patient population and druggability of the partner gene. From an initial 5 billion possible gene pairs, 4,332 statistically significant SLI candidates were identified, which were then refined to a set of 142 high-confidence, actionable SLIs based on effect size, targetability, and clinical relevance filters.

Figure 2. Potential synthetic lethal interactions across cancer types.

The heatmap displays the top 10 most significant SLIs identified for each cancer type in the analysis. The red color scale corresponds to the delta dependency (DD) score, representing the difference in gene essentiality between the mutant and wildtype groups. The blue bar at the bottom indicates the number of cancer types where the SLI was determined as statistically significant. SLIs with P $<0.001, aremarkedwithanasterisk.$

Figure 3. Validation of predicted synthetic lethal interactions against STRING-db database.

Bar plots show the percentage of gene pairs from the SLAYER analysis that exhibited evidence of interaction or co-occurrence in the STRING-db database, which integrates known and predicted protein associations from multiple sources. The blue bars represent the percentages for the 142 high-confidence SLIs identified by SLAYER, while the red bars indicate the background percentages when analyzing all possible pairwise combinations of driver genes and genes across the different cancer types.

Figure 4. Potential synthetic lethal interactions in bladder cancer.

A. Heatmap depicting the top synthetic lethal interaction (SLI) pairs in bladder cancer, with redder colors indicating higher delta dependency scores. **B.** Volcano plot showing all potential synthetic lethal interactions for the RB1 mutation, with AHR and CDK2 identified as the top-ranking candidates based on delta dependency (x-axis) and statistical significance (-log10 p-value on y-axis). **C.** Boxplots illustrating the separation in gene dependency scores between RB1 wild-type and RB1 mutant bladder cancer cell lines for the AHR and CDK2. **D.** Dependency network for AHR in bladder cancer, highlighting edges that connect these genes to RB1-associated pathways. **E.** Correlation plot between the dependency scores of AHR and the enrichment of RB1-related pathway across the cell lines.

Figure 5. Synthetic lethality between RB1 and AhR in bladder cancer.

A. Short-term cell viability assay in T24 and 5637 cells treated with increasing concentrations of BAY-2416964. Cell viability was measured 24 hr after drug treatment. Data are presented as mean ± s.d. (n=3). *P $<$ 0.05;**P $<$ 0.01;***P $<$ 0.001 . **B.** Short-term cell viability assay in p53 WT and p53 null RPE1-hTERT cells treated with increasing concentrations of BAY-2416964. Cell viability was measured 24 hr after drug treatment. Data are presented as mean ± s.d. (n=3). **C.** Short-term cell viability assay in T24 cells expressing either scramble shRNA or shRNA targeting Rb1 and treated with increasing concentrations of BAY-2416964. Cell viability was measured 72 hr after drug treatment. Data are presented as mean ± s.d. (n=3). **D.** Quantitative RT-qPCR analysis of Rb1 knockdown in indicated T24 cell lines. ****P $<$ 0.0001.